Comparative transcriptomic analysis reveals the cold acclimation during chilling stress in sensitive and resistant passion fruit (*Passiflora edulis)* cultivars

Yanyan Wu [1] , **Weihua Huang** [1] , **Qinglan Tian** [1] , **Jieyun Liu** [1] , **Xiuzhong Xia** [2] , **Xinghai Yang** [Corresp., 2] , **Haifei Mou** [Corresp. 1]

[1] Biotechnology Research Institute, Guangxi Academy of Agricultural Sciences, Nanning, Guangxi, CHINA

[2] Rice Research Institute, Guangxi Academy of Agricultural Sciences, Nanning, Guangxi, CHINA

Corresponding Authors: Xinghai Yang, Haifei Mou
Email address: yangxinghai888@gxaas.net, mhf@gxaas.net

Chilling stress (CS) is an important limiting factor for the growth and development of passion fruit (*Passiflora edulis*) in winter in south China. However, little is known about how the passion fruit responds and adapts to CS. In this study, we performed transcriptome sequencing of Huangjinguo (HJG, cold-susceptible) and Tainong 1 (TN1, cold-tolerant) under normal temperature (NT) and CS conditions, and a total of 47,353 unigenes were obtained in 7 databases. Using differentially expressed unigenes (DEGs) analysis, 3,248 and 4,340 DEGswere identified at two stages, respectively. The Gene Ontology (GO) enrichment analysis showed that the DEGs were mainly related to phosphorylation, membrane protein, and catalytic activity. In Kyoto Encyclopedia of Genes and Genomes (KEGG) pathway, the unigenes of plant-pathogen interaction, plant hormone signal transduction and fatty acid metabolism were enriched.Then, the 12,471 filtered unigenes were divided into 8 co-expression modules, and two of which were correlated with CS. In the two modules, 32 hub unigenes were obtained. Furthermore, the unigenes related to CS were validated using quantitative real-time PCR (RT-qPCR). This work showed that the expression levels of CS-related unigenes were very different in two passion fruit cultivars. The results provide information for the development of passion fruit with increased chilling tolerance.

1 **Title: Comparative transcriptomic analysis reveals the cold acclimation**

2 **during chilling stress in sensitive and resistant passion fruit (*Passiflora edulis)***

3 **cultivars**

4 Yanyan Wu[1], Weihua Huang[1], Qinglan Tian[1], Jieyun Liu[1], Xiuzhong Xia[2], Xinghai Yang[2*],

5 Haifei Mou[1*]

6 [1]Biotechnology Research Institute, Guangxi Academy of Agricultural Sciences, Nanning,

7 Guangxi 530007, China

8 [2]Rice Research Institute, Guangxi Academy of Agricultural Sciences, Nanning, Guangxi 530007,

9 China

10 ***Corresponding author**: Xinghai Yang; **Department/Institute**: Rice Research Institute,

11 Guangxi Academy of Agricultural Sciences; **Address**: 174 East Daxue Road, Nanning, Guangxi

12 530007, Chian; **E-mail**: yangxinghai514@163.com; Tel: +867713244040; ORCID ID:

13 https://orcid.org/0000-0002-3476-2578.

14 ***Co-corresponding author**: Haifei Mou; **Department/Institute**: Biotechnology Research

15 Institute, Guangxi Academy of Agricultural Sciences; **Address**: 174 East Daxue Road, Nanning,

16 Guangxi 530007, China; **E-mail**: mhf@gxaas.net; Tel: +86771 3243531

Abstract

Chilling stress (CS) is an important limiting factor for the growth and development of passion

fruit (*Passiflora edulis*) in winter in south China. However, little is known about how the passion

fruit responds and adapts to CS. In this study, we performed transcriptome sequencing of

Huangjinguo (HJG, cold-susceptible) and Tainong 1 (TN1, cold-tolerant) under normal

temperature (NT) and CS conditions, and a total of 47,353 unigenes were obtained in 7 databases.

Using differentially expressed unigenes (DEGs) analysis, 3,248 and 4,340 DEGswere identified

at two stages, respectively. The Gene Ontology (GO) enrichment analysis showed that the DEGs

were mainly related to phosphorylation, membrane protein, and catalytic activity. In Kyoto

Encyclopedia of Genes and Genomes (KEGG) pathway, the unigenes of plant-pathogen

interaction, plant hormone signal transduction and fatty acid metabolism were enriched.Then, the

12,471 filtered unigenes were divided into 8 co-expression modules, and two of which were

correlated with CS. In the two modules, 32 hub unigenes were obtained. Furthermore, the

unigenes related to CS were validated using quantitative real−time PCR (RT-qPCR). This work

showed that the expression levels of CS-related unigenes were very different in two passion fruit

cultivars. The results provide information for the development of passion fruit with increased

chilling tolerance.

Key words Passion fruit, Chilling stres, RNA-seq, WGCNA, Hub genes, RT-qPCR

Introduction

Passion fruit is a tropical and subtropical fruit tree that is widely planted in south China and its

fruit has an aromatic smell and high nutritional values. But passion fruit is susceptible to cold

stress in winter (Liu et al. 2017A), which can cause large economic loss.

Cold stress is one of the limiting factors for plant growth and development (Shi et al. 2018). In

plants, cold stress is classified into chilling stress (0-15 $^\circ$C) and freezing stress (<0 $^\circ$C) (Yadav

2010; Shi et al. 2018). The cold environment can cause changes in the structure and activity of

54 proteins in plant cells, leading to altered enzymatic reactions such as photosynthesis and

55 respiration, and eventually leading to symptoms such as wilting and yellowing of plant leaves

56 (Hendrickson et al. 2006). When plants are in reproductive growth, cold stress can cause damage

57 of the plant reproductive organs, and the seed setting rate will be significantly reduced, which

58 will eventually affect crop yields and cause major losses to agricultural production. Plants can

59 gain resistance to low temperature,and this process is called cold acclimation. The cold

60 acclimation of plants includes changes in a variety of intracellular physiological and biochemical

61 processes. The most significant changes include the instantaneous increase of calcium ion

62 concentration (Carpaneto et al. 2007), growth cessation, decrease in tissue water content affect

63 plant hormones abscisic acid (ABA), brassinolide (BR), and gibberellin (GA), cause fatty acid

64 unsaturation and lipid peroxidation (Hara et al. 2003), changes in phospholipid composition

65 (Webb et al. 1994), and osmotic pressure such as proline, betaine and soluble sugar (Krasensky

66 et al. 2012). The molecular mechanism of cold acclimation is that non-freezing low temperature

67 can induce plants to express a series of cold response proteins to help plants resist freezing at low

68 temperature. Inducer of CBF expression (ICE)- C-repeat binding factors (CBF)- cold-regulated

69 proteins (COR) is thought to be one of the most important defense pathways in plants against

70 cold stress (Shi et al. 2018). CBF can regulate the expression of COR by binding to the C-

71 repeat/dehydration-responsive element (CRT/DRE) sequence that resides in the promoter region

72 of the *COR* gene (Stockinger et al. 1997; Liu et al. 1998). ICE1 is located upstream of *CBF*, and

73 it is a MYC-like bHLH type transcription factor, which can bind to the recognition site of the

74 *CBF3* promoter and regulate its expression (Chinnusamy et al. 2003) Moreover, some CBF-

75 independent transcription factors are involved in modulating COR expression, and various

76 transcription factors, including CAMTA3 (Doherty et al. 2009), ZAT12 (Vogel et al. 2005), and

77 HY15 (Catalá et al. 2011) can regulate the expression of CBFs. Protein phosphorylation also

78 plays an important role in regulating the response of plants to low temperature (Mann m 2003),

79 and mitogen-activated protein kinase (MAPK) as an important element in signal transmission

80 (Zhao et al. 2017A).

81   Guangxi belongs to a tropical and subtropical monsoon climate. The coldest month in January

82   has an average daily temperature of 5.5°C to 15.2°C. The continuous low temperature in winter

83   affects the growth of passion fruit. However, no systematic study on the CS of passion fruit has

84   been reported. In this study, the RNA-seq data was used to analyze gene expression during CS in

85   passion fruit cultivars Huangjinguo (HJG) and Tainong1 (TN1). The main aims to (i) analyze the

86   gene expression profile of passion fruit during CS, (ii) explore the functions of differentially

87   expressed unigenes (DEGs), (iii) construct regulation network of the interactions of chilling

88   tolerance genes of passion fruit, (iv) identify the hub genes that affect the CS of passion fruit.

89   **Materials and Methods**

90   **Plant materials**

91   HJG was introduced in the Bannahuangguo of Xishuangbanna Botanical Garden in Yunnan, and

92   it is a cold-sensitive accession. TN1 comes from Taiwan, and it is a cold-resistant purple passion

93   fruit. The cutting seedling heights ranged from 29 to 38 cm, and the seedlings were transplanted

94   in Nanning experimental field (Guangxi, China, 22.85 ˚N, 108.26 ˚E) on May 25, 2019. The first

95   sampling time was November 25th, 2019, at 10 am in the morning, and the temperature was 25

96   ᵒC. The second sampling time was January 18, 2020, at 10 am in the morning, and the

97   temperature was 7 ᵒC. The fresh leaves of passion fruit were snap frozen in liquid nitrogen, and

98   then stored in -80 ᵒC freezer. Each sample had three biological replicates. Under NT condition,

99   the three biological replicates of HJG, HJGA1, HJGA2 and HJGA3, were recorded as A1; the

100 three biological replicates of TN1, TN1A1, TN1A2 and TN1A3 were recorded as A2. Under CS

101 condition, three biological replicates of HJG, HJGB1, HJGB2 and HJGB3, were denoted as B1;

102 three biological replicates of TN1, TN1B1, TN1B2 and TN1B3, were denoted as B2.

103 **RNA extraction, sequencing, assembly and annotation**

104 Total RNA was extracted with RNAprep Pure kit (Tiangen, Beijing, China) according to the

105 manufacturer's instructions. Nanodrop2000 (Shimadzu, Japan) was used to detect the

106 concentration and purity of the extracted RNA. Agarose gel electrophoresis was used to detect

107 the integrity of the RNA, and Agilent 2100 (Agilent, America) was used to determine the RIN

108 value. A single library requires 1μg of RNA, with a concentration of ≥ 50 ng/μL, and

109 OD260/280 between 1.8 and 2.2. Magnetic beads (Invitrogen, America) with Oligo (dT) was

110 used to pair with the 3' poly A tail of eukaryotic mRNA, thus isolating mRNA from total RNA.

111 Subsequent, reverse synthesis of cDNA was performed. These libraries above were sequenced

112 using an Illumina NovaSeq 6000 sequencer (Illumina Inc., USA) and 150 bp paired-end reads

113 were generated. In order to ensure the accuracy of subsequent analysis, the original sequencing

114 data were filtered first to obtain clean data.

115   We used Trinity v2.8.6 (Haas et al. 2013) to splice the transcript fragments to obtain

116 transcripts, and then used CD-HIT to cluster the transcript sequences to remove redundant

117 sequences and get all the unigene sequence sets for the subsequent analysis. Bowtie 2 (Salzberg

118 et al. 2012) was used to align the sequencing data to the reconstructed unigene sequence set, and

119 the alignment file was mainly used for subsequent unigene quantification and differential

120 expression analysis. The unigene sequences were compared with the NCBI non-redundant

121 protein sequences (NR), Swiss-Prot, TrEMBL, KEGG, GO, Pfam, and EuKaryotic Orthologous

122 Groups (KOG) databases using Basic Local Alignment Search Tool (BLAST). Finally,

123 HMMER3 (Finn et al. 2011) was used to align the amino acid sequence of unigene with the

124 Pfam database to obtain the annotation information of unigenes.

125 **Enrichment analysis of DEGs**

126 The read counts and transcripts per million reads (TPM) were calculated using RSEM (Li et al.

127 2011) and bowtie2 (Salzberg et al. 2012). The DEGs were identified through the software

128 packages of Bioconductor 3.11-DESeq2 (Love et al. 2014). The screening threshold is false

129 discovery rate (FDR) < 0.05, and log2 fold change (FC (condition 2/condition 1) for a gene) > 1

130 or log2FC < -1. The DEGs were classified, and GO and KEGG enrichment analysis were was

131 subsequently performed.

132 **Weighted gene co-expression network analysis**

133 We followed these steps below for weighted gene co-expression network analysis (WGCNA): (i)

134 screening DEGs for WGCNA cluster analysis; (ii) calling the R package to cluster the DEGs; (iii)

135   calling ggplot2 in the R package to draw the clustering heat map and histogram of each module;

136   (iv) using the topGO to perform GO enrichment analysis on each module; (v) calling Fisher-test

137   function in R for KEGG enrichment analysis; (vi) using Cytoscape3.8.0 (Su et al. 2014) to draw

138   network diagram. A signed network was constructed usingthe blockwiseModules function, with

139   the following parameters: power = 14, minModuleSize = 30,mergeCutHeight = 0.25,corType

140   = pearson. When co-expressed genes are defined according to the above-mentioned standards,

141   each gene is assigned a module number and corresponding module color; otherwise use the 'gray'

142   module.

143   **Validation of the CS-related genes using RT-qPCR**

144   We selected 11 genes related to plant hormone signaling, fatty acid metabolism and plant-

145   pathogen interaction using GO and KEGG database, and 4 hub genes in WGCNA for validation.

146   The primers were designed using Primer3 (Table S1). Using *HIS* as the reference gene (Liu et al.

147   2017A), RT-qPCR was used to analyze the expression level of 15 genes in B1 and B2.

148   The identical RNA samples as RNA-seq experiments were used for RT-qPCR analysis. The

149   detailed experimental method refers to Wu et al. (Wu et al. 2020). The relative gene expression

150   level was calculated by reference to the $2^{-\Delta\Delta Ct}$ method (Livak et al. 2001). All unigenes

151   expression analysis were performed in triplicates. The values represented arithmetic averages of

152   three replicates, and the data were expressed as a mean plus and minus standard deviation

153   (mean ± SD).

154   **Statistical analysis**

155   CASAVA was used for base calling. Subsequently, we used SeqPrep for quality control of raw

156   sequencing data. Pearson correlation coefficient is used to measure the correlation between

157   samples. The package heatmap of R was used to prepare the correlation between samples and

158   DEGs expression pattern clustering. Data of RT-qPCR was analyzed using Excel 2007. The

159   figures were prepared using Origin 9.65.

160   **Results**

161   **Quality control and assembly of passion fruit transcriptome sequences**

162 To compare gene expression profiles of the two passion fruit cultivars under NT and CS,

163 transcriptome sequencing and analysis were performed. After decontamination and adaptor

164 removal, 533,935,574 raw reads were obtained from 12 samples, a total of 80.09 Gb clean reads

165 and 6.67 Gb per sample. The Q30 base percentage was 93.22% and GC content was 44.64%

166 (Table 1).

167 The clean reads were assembled into transcripts using the Trinity in paired-end method, and

168 211,874 transcript were obtained.The CD-HIT was then used to cluster the transcripts, which

169 yielded 47,353 unigenes with an average length of N50 of 2,368 bp, N90 of 450 bp, and an

170 average length of 1,211 bp. Afterwards, Bowtie2 was used to align the sequences of each sample

171 to the unigene sequence set, with an average alignment ratio of 77.89% (Table 2).

172 **Unigene function annotation**

173 The assembled unigenes were annotated to databases including the NR, Swiss-Prot, TrEMBL,

174 KEGG, GO, Pfam, and KOG, to which 97.92%, 70.40%, 97.82%, 33.97%, 36.16%, 61.43%, and

175 48.92% of unigenes were mapped, respectively. A total of 47,353 unigenes acquired annotation

176 information (Table 3). The number of annotated unigenes in NR and TrEMBL was the largest,

177 which were 46,369 and 46,323, respectively.

178 In GO database, 17,123 unigenes were annotated and matched to three major categories:

179 biological process (BP), cellular component (CC) and molecular function (MF). Enriched BP

180 terms were mainly about "metabolic process" (4,350) and "cellular process" (2,191). Enriched

181 CC terms were mainly about "membrane part" (1,270) and "cell part"(890). Enriched MF terms

182 were mainly about "binding" (7,367)and "catalytic activity" (5,715) (Fig. 1A).

183 In KOG database, 23,164 unigenes were annotated, which were clustered into 25 categories.

184 The unigenes were mainly about "signal transduction mechanisms" (2,439) and

185 "posttranslational modification, protein turnover, chaperones" (2,138) (Fig. 1B).

186 In KEGG database, 16,086 unigenes were annotated. According to the functions, these

187 unigenes were enriched in 9 pathways. The enriched pathways were mainly about "metabolism"

188 (10,045) and "organismal systems" (4,505) (Fig. 1C).

189 **Comparative analysis of DEGs in two cultivars at two stages**

190 In order to gain insights on the adaptation of passion fruit to CS, the TPM method was used to

191 analyze the gene expression levels in the two stages (Fig. S1). The correlation coefficient

192 between the three biological replicates was 0.87 in HJGA, 0.98 in TN1A, 0.96 in HJGB, 0.99 in

193 TN1B, and the average correlation coefficient value was 0.95 (Fig. S2), indicating that the

194 reproducibility of this study was good and the experimental results were reliable.

195 The software package DESeq2 was used to perform differential expression analysis of

196 unigenes. There were 3,248 and 4,340 DEGs at two stages, respectively. After, analysis of the

197 DEGs for the two stages, we found that the DEGs between HJG and TN1 were increased by 33.6%

198 under CS condition (1,092), and 87.5% (955) were up-regulated (Fig. 2A).

199 Cluster analysis of gene expression can intuitively reflect the level of gene expression and

200 expression patterns in multiple samples. We used the DEGs to perform cluster analysis on A1 vs

201 A2 (Fig. 2B) and B1 vs B2 (Fig. 2C). The results showed that the difference between the three

202 biological replicates of each group was small, which again confirmed the rationality of sample

203 selection.

204 **GO and KEGG pathway enrichment analysis of DEGs**

205 There were 1,182 up-regulated unigenes, and 2,066 down-regulated unigenes at stage A; and

206 there were 2,137 up-regulated unigenes and 2,203 down-regulated unigenes at stage B.

207 GO enrichment analysis indicated that "metabolic process" (542), "oxidation-reduction

208 process" (156), "protein phosphorylation" (92), "carbohydrate metabolic process"(73), "organic

209 substance catabolic process" (40), and "catabolic process" (40), "extracellular region" (10),

210 "apoplast" (8), "cell wall" (8), "external encapsulating structure" (8), "catalytic activity" (634),

211 "transferase activity" (228), "oxidoreductase activity" (167), "metal ion binding" (146), "cation

212 binding" (146), and "transition metal ion binding" were enriched at stage A (110) (Table S2).

213 But "oxidation-reduction process" (187), "phosphate-containing compound metabolic process"

214 (171), "phosphorus metabolic process" (171), "macromolecule modification" (170), "cellular

215 protein modification process" (169), and "protein modification process" (169), "membrane"

216 (213), "intrinsic component of membrane" (99), and "integral component of membrane"

217 (97),"catalytic activity" (837), "transferase activity" (326), "cation binding" (202), "metal ion

218 binding" (201), "oxidoreductase activity" (198), "phosphotransferase activity", and "alcohol

219 group as acceptor" (165) were enriched at stage B (Table S3).

220 The GO terms in A (P> 0.05) were compared to B (P ≤ 0.05), and the unigenes were mainly

221 about "protein phosphorylation" (GO:0006468 , 61) "phosphorylation" (GO:0016310, 61),

222 "response to stimulus" (35), "lipid metabolic process" (19), "response to chemical" (13),

223 "membrane" (73), "intrinsic component of membrane" (29), "integral component of membrane"

224 (28) "catalytic activity", "acting on a protein" (77), "transferase activity", "transferring

225 phosphorus-containing groups" (70), "kinase activity" (67), "phosphotransferase activity",

226 "alcohol group as acceptor" (67), and "protein kinase activity" (62) (Table S4).

227 The KEGG pathway enrichment analysis can reveal the main metabolic pathways and signal

228 transduction pathways in which the DEGs were involved, and the prevailing pathways were as

229 follows: "ribosome" (42), "carbon metabolism" (39), "biosynthesis of amino acids" (30), "starch

230 and sucrose metabolism" (21), "and cysteine and methionine metabolism" (20) at stage A; "plant

231 hormone signal transduction" (31), "plant-pathogen interaction" (27), "fatty acid metabolism"

232 (21), "cysteine and methionine metabolism" (20) (Fig. 3A). The KEGG pathway in A (P> 0.05)

233 were compared to B (P ≤ 0.05), and the unigenes were mainly about "plant-pathogen interaction"

234 (17), "plant hormone signal transduction" (14), and "fatty acid metabolism" (8) (Fig. 3B).

235 **WGCNA analysis**

236 After background correction and normalization of the unigenes expression data, we filtered out

237 the abnormal and minor changed unigenes. Finally, we obtained 12,471 highly expressed

238 unigenes (Table S5). In this study, when the soft threshold was 16 (Fig. S3), the gene topology

239 matrix expression network was closest to the scale-free distribution. A gene cluster tree was

240 constructed based on the correlation between genes, and each branch corresponded to a cluster of

241 gene sets with highly correlated expression levels (Fig. S4a).

242 According to the standard of mixed dynamic shear, the gene modules were classified and the

243 eigenvector of each module was calculated. The modules close to each other were merged, and 8

244 co-expression modules were obtained (Fig. S4b). Each module used different colors to represent

245 the clustered genes. The turquoise module had the most clustered genes (4,171), the red module

246 contained the fewest (81), and the grey module contained the unigenes that couldn't be included

247 in any module.

248 The DEGs were used to draw the heat map of each module in the four sample groups. The

249 brown and yellow modules showed less changes in differential unigenes between the early and

250 late HJG, but showed larger changes in differential unigenes between early and late TN1 (Fig.4),

251 which is consistent with the chilling resistance feature of TN1. Therefore, we selected the

252 unigenes of these two modules for in-depth GO and KEGG pathway analysis.

253 In the brown module, the significant terms in GO database were "cellular macromolecule

254 metabolic process", "phosphate-containing compound metabolic process", "phosphorus

255 metabolic process", "protein phosphorylation", "stimulus", "transferase complex", "riboflavin

256 synthase complex", "photosystem I reaction center", "photosystem I""binding", "metal ion

257 binding", "cation binding", "phosphotransferase activity", "alcohol group as acceptor", "kinase

258 activity" (Table S6). In the KEGG pathway analysis, the prevailing pathways were "plant

259 hormone signal transduction", "MAPK signaling pathway", and "starch and sucrose metabolism"

260 (Fig. 5A).

261 In the yellow module, the GO significant terms in GO database   were "cellular process",

262 "macromolecule modification", "phosphorus metabolic process", "cellular protein modification

263 process", "protein modification process", "cell periphery", "photosystem", "photosynthetic

264 membrane", "thylakoid", "extracellular region", "3-deoxy-7-phosphoheptulonate synthase

265 activity", "alkylbase DNA N-glycosylase activity", "DNA-3-methyladenine glycosylase

266 activity", "DNA N-glycosylase activity", and "method adenosyltransferase activity" (Table S7).

267 The significantly enriched pathways included "biosynthesis of amino acids", "plant hormone

268 signal transduction", "ABC transporters", "starch and sucrose metabolism", "folate biosynthesis"

269 and "other pathways" that might be related to CS (Fig. 5B).

270   The constructed network was visualized with the Cytoscape in the brown and yellow modules,

271   and got 19 hub unigenes which mainly related to "MAPK signaling pathway", "plant hormone

272   signal transduction", "starch and sucrose metabolism", "fatty acid biosynthesis" and

273   "photosynthesis in the brown module" (Fig. 6A). In the yellow module, 13 hub unigeneswere

274   mainly related to "plant hormone signal transduction", "MAPK signaling pathway", "starch and

275   sucrose metabolism", and "fatty acid degradation" (Fig. 6B).

276   **Validation of gene expression changes during chilling acclimation**

277   We used the RT-qPCR method to validate the expression level of 15 unigenes. The results

278   showed that the RT-qPCR expression patterns of the 15 unigenes were consistent with RNA-seq

279   analysis (Fig. 7, Table S8). RT-qPCR analysis showed that the 9 unigenes were ≥2 or ≤0.5 fold-

280   change. Comparison with B1 and B2, TPM value of 12 unigenes were ≥2 or ≤0.5 fold-change.

281   The results showed that seventy-five percent DEGs could be validated using RT-qPCR, and

282   DEGs analysis were highly reliable.

283   **Discussions**

284   Low temperature is one of the main abiotic stresses that the plants are vulnerable to during their

285   life cycle, and the response of plants to low temperature stress is a multi-factor synergistic

286   process involving complex physiological and gene expression regulatory networks. With the

287   development of molecular biology technology, researchers have cloned many low temperatur

288   related genes in *Arabidopsis thaliana* (Wang et al. 2019; Ding et al. 2018; Ye et al. 2019) and

289   rice (Ma et al. 2015; Zhang et al. 2017A) . Passion fruit is a tropical and subtropical fruit tree and

290   it is vulnerable to low temperature in winter. However, there are fewer studies on cold stress in

291   passion fruit. In this study, the passion fruit cultivar of 'Tainong 1' was identified, which has the

292   characteristics of cold-tolerance.

293   Although the two cDNA libraries were constructed for transcriptome sequencing in passion

294   fruit under CS condition (Liu et al. 2017A), we still know little about the cold tolerance of

295   passion fruit. To reveal the expression pattern of CS-related genes in passion fruit, RNA-seq

296   analysis were performed. Using database function annotation, we obtained 47,353

297   unigenes.Based on RNA-seq data, the number of down-regulated DEGs did not change much at

298   two stages, but the number of up-regulated differential unigenes were 955, indicating that the up-

299   regulation of DEGs maybe related to CS.

300   Protein phosphorylation is also a type of post-translational regulation during the cold

301   acclimation in plant. Under cold condition, CRPK1 is activated and phosphorylates 14-3-3λ, and

302   the phosphorylated 14-3-3λ enters nucleus from the cytoplasm and degrades CBFs via direct

303   interaction in *Arabidopsis* (Liu et al. 2017B). Transcriptome sequencing reveaeled that 61 DEGs

304   of phosphorylation were significantly up-regulated or down-regulated in the two stages,

305   respectively (Table S4). Furthermore, the unigenes were mainly related to calcium-dependent

306   protein kinase, serine/threonine-protein kinase, and CBL-interacting serine/threonine-protein

307   kinase. In rice, calcium-dependent protein kinase gene OsCPK17 (Almadanim et al. 2018),

308   OsCDPK7 (Saijo et al. 2000) and OsCPK24 (Liu et al. 2018B) all respond to low temperature. In

309   a previous study, serine/threonine protein kinase reponsed to cold stress (Soto et al. 2002). These

310   results indicated that protein phosphorylation could play an important role in cold acclimation of

311   passion fruit.

312   Mitogen-activated protein kinase (MAPK) plays an important role in signal transduction, and

313   is also essential for regulating the cold response of plants.Under low temperature, the

314   phosphorylation levels of MPK3, MPK4 and MPK6 were significantly increased (Zhao et al.

315   2017B); moreover, MPK3 and MPK6 could interact with ICE1 to participate in low-temperature

316   response (Li et al. 2017). Zhang et al. found that the phosphorylated OsICE1 could promote

317   *OsTPP1* transcription and induce the production of large amounts of trehalose, thereby

318   improving the cold resistance of rice (Zhang et al. 2017B). Using WGCNA analysis, we found

319   that MAPK signaling pathway significantly enriched in the brown module, which contained 7

320   DEGs (Fig. 5A). Moreover, the functional annotation of *TRINITY_DN36339_c2_g1_i5* was

321   mitogen-activated protein kinase kinase kinase 3. In rice, OsMKK6 and OsMPK3 constitute a

322   moderately low-temperature signalling pathway and regulate cold stress tolerance (Xie et al.

323   2012). MKK2 induces the expression of COR genes to enhance the freezing tolerance of

324   *Arabidopsis* (Teige et al. 2004).

325   In plants, hormones and cold signaling pathways are coordinated to better adapt to cold stress.

326   ABA is used as an important signal molecule and the most important stress signal in hormones,

327   and it can mediate the signal transduction pathway to cold stress and increase the tolerance of

328   cold stress (Yuan et al. 2018B). Auxin acts as a trigger in plant growth and development. In rice,

329   ROC1 can regulate *CBF1*, and auxin can affect ROC1 levels (Dou et al. 2016). In addition, BR,

330   GA, JA, ethylene, CK, and melatonin play important regulatory roles in the ICE–CBF–COR

331   pathway (Wang et al. 2017). In CS condition, we found 31unigenes about plant hormone signal

332   transduction (Fig. 3A). In WGCNA analysis, the pathway of plant hormone signal transduction

333   was enriched in brown and yellow modules. These unigenes were annotated about aux, JA, ABA ,

334   and BR.

335   Plants use fatty acid dehydrogenase to regulate the increase of fatty acid unsaturation to

336   improve the cold resistance (Upchurch 2008; He et al. 2015). The change of malondialdehyde

337   content caused by lipid peroxidation is negatively correlated with plant cold resistance (Kim et al.

338   2011). In this study, the unigenes related to fatty acid metabolism and lipid metabolic process

339   were identified (Fig. 3A, Fig. 6B). Among them, 16 unigenes were annotated as delta(12)-fatty-

340   acid desaturase (FAD2). In rice, *OsFAD2* is involved in fatty acid desaturation and maintenance

341   of the membrane lipids balance in cells, and could improve the low temperature tolerance (Shi et

342   al. 2012). Similarly, *FAD2* could improve the salt tolerance during seed germination and early

343   seedling growth (Zhang et al. 2012), but *FAD8* was strongly inducible by low temperature in

344   *Arabidopsis thaliana* (Gibson et al. 1994). The results indicated that *FAD2* could improve the CS

345   of passion fruit.

346   In the process of cold acclimation in plants, the hydrolysis of starch is intensified and the

347   content of soluble sugar increases.As a result, the freezing point of cell fluid is lowered and the

348   excessive dehydration of cells is reduced (Krasensky j 2012; Yue et al. 2015). The analysis of

349   pathway enriched by KEEG and WGCNA revealed starch and sucrose metabolism related to

350   cold stress was enriched at stage B. Three DEGs were obtained at stage B compare to stage A,

351 and these unigenes were annotated as beta-glucosidase and glucan endo-1,3-beta-glucosidase 3-

352 like genes.

353 **Conclusions**

354 In this study, we performed a comprehensive comparative transcriptome analysis firstly

355 between two passion fruit cultivars, to idenfy the gene expression level and analyze molecular

356 mechanism of CS. This work showed that the unigenes of protein phosphorylation, MAPK

357 signaling, plant hormones and fatty acid metabolism play important roles in the hilling tolerance

358 between the two passion fruit cultivars. Furthermore, 32 hub unigenes were assigned to two

359 modules, which could played a vital role in the chilling acclimation of passion fruit. In all, these

360 findings provide a deepened understanding of the molecular mechanism of cold stress and could

361 facilitate the genetic improvement of chilling tolerance in passion fruit.

362 **Acknowledgments**

363 The authors thank to Dr. Yinghua Pan for help providing data analysis suggestions.

364 **References**

365 **Almadanim MC, Gonçalves NM, Rosa M, Alexandre BM, Cordeiro AM, Rodrigues M, Saibo N, Soares**

366 **CM, Romão CV, Oliveira MM, Abreu IA. 2018.** The rice cold-responsive calcium-dependent protein

367 kinase OsCPK17 is regulated by alternative splicing and post-translational modifications. Biochim

368 Biophys Acta Mol Cell Res **1865**: 231-246.

369 **Carpaneto A, Ivashikina N, Levchenko V, Krol E, Jeworutzki E, Zhu J, Hedrich H. 2007.** Cold

370 transiently activates calcium-permeable channels in *Arabidopsis* mesophyll cells. Plant Physiol **143**: 487-

371 494.

372 **Catalá R, Medina J, Salinas J. 2011.** Integration of low temperature and light signaling during cold

373 acclimation response in *Arabidopsis*. Proc Natl Acad Sci U S A **108**: 16475-16480.

374 **Chinnusamy V, Ohta M, Kanrar S, Lee BH, Hong X, Agarwal M, Zhu JK. 2003.** ICE1: a regulator of

375 cold-induced transcriptome and freezing tolerance in *Arabidopsis*. Genes Dev **17**: 1034-1054.

376 **Ding Y, Jia Y, Shi Y, Zhang X, Song C, Gong Z, Yang S. 2018.** OST1-mediated BTF3L phosphorylation

377 positively regulates CBFs during plant cold responses. EMBO J **37**: e98228.

378 **Doherty CJ, Van buskirk HA, Myers SJ, Thomashow MF. 2009.** Roles for *Arabidopsis* camta transcription

379 factors in cold-regulated gene expression and freezing tolerance. Plant Cell **21**: 972-984.

380 **Dou M, Cheng S, Zhao B, Xuan Y, Shao M. 2016.** The indeterminate domain protein ROC1 regulates

381 chilling tolerance via activation of DREB1B/CBF1 in rice. Int J Mol Sci **17**: 233.

382 **Finn RD, Clements J, Eddy SR. 2011.** HMMER web server: interactive sequence similarity searching.

383 Nucleic Acids Res **39**: W29-W37.

384 **Gibson S, Arondel V, Iba K, Somerville C. 1994.** Cloning of a temperature-regulated gene encoding a

385 chloroplast ω-3 desaturase from *Arabidopsis* thaliana. Plant Physiol **106**: 1615-1621.

386   **Guo X, Liu D, Chong K. 2018.** Cold signaling in plants: Insights into mechanisms and regulation. J Integr
387   Plant Biol **60**: 745-756.
388   **Haas BJ, Papanicolaou A, Yassour M, Grabherr M, Blood PD, Bowden J, Couger MB, Eccles D, Li B,**
389   **Lieber M, Macmanes MD, Ott M, Orvis J, Pochet N, Strozzi F, Weeks N, Westerman R, William T,**
390   **Dewey CN, Henschel R, Leduc RD, Friedman N, Regev A. 2013.** De novo transcript sequence
391   Reconstruction from RNA-seq using the Trinity platform for reference Generation and analysis. Nat
392   Protoc **8**: 1494-1512.
393   **Hara M, Terashima S, Fukaya T, Kuboi T. 2003.** Enhancement of cold tolerance and inhibition of lipid
394   peroxidation by citrus dehydrin in transgenic tobacco. Planta **217**: 290-298.
395   **He J, Yang Z, Hu B, Ji X, Wei Y, Lin L, Zhang Q. 2015.** Correlation of polyunsaturated fatty acids with the
396   cold adaptation of Rhodotorula glutinis. Yeast **32**: 683-690.
397   **Hendrickson L, Vlcková A, Selstam E, Huner N, Oquist G, Hurry V. 2006.** Cold acclimation of the
398   *Arabidopsis* dgd1 mutant results in recovery from photosystem I-limited photosynthesis. FEBS Lett **580**:
399   4959-4968.
400   **Kim SI, Tai TH. 2011.** Evaluation of seedling cold tolerance in rice cultivars: a comparison of visual ratings
401   and quantitative indicators of physiological changes. Euphytica **178**: 437-447.
402   **Kim SH, Kim HS, Bahk S, An J, Yoo Y, Jy K, Chung WS. 2017.** Phosphorylation of the transcriptional
403   repressor MYB15 by mitogen-activated protein kinase 6 is required for freezing tolerance in *Arabidopsis*.
404   Nucleic Acids Res **45**: 6613-6627.
405   **Krasensky J, Jonak C. 2012.** Drought, salt, and temperature stress-induced metabolic rearrangements and
406   regulatory networks. J Exp Bot **63**: 1593-1608.
407   **Krishnan N, Dickman MB, Becker DF. 2008.** Proline modulates the intracellular redox environment and
408   protects mammalian cells against oxidative stress. Free Radic Biol Med **44**: 671-681.
409   **Li H, Ding YL, Shi YT, Zhang XY, Zhang SQ, Gong ZZ, Yang SH. 2017.** MPK3- and MPK6-mediated
410   ICE1 phosphorylation negatively regulates ICE1 stability and freezing tolerance in *Arabidopsis*. Dev Cell
411   **43**: 630-642.
412   **Li B, Dewey CN. 2011.** RSEM: accurate transcript quantification from RNA-Seq data with or without a
413   reference genome. BMC Bioinformatics **12**: 323.
414   **Liu Q, Kasuga M, Sakuma Y, Abe H, Miura S, Yamaguchi-shinozaki K, Shinozaki K. 1998.** Two
415   transcription factors, DREB1 and DREB2, with an EREBP/AP2 DNA binding domain separate two
416   cellular signal transduction pathways in drought- and low-temperature-responsive gene expression,
417   respectively, in *Arabidopsis*. Plant Cell **10**: 1391-1406.
418   **Liu S, Li AD, Chen CH, Cao GJ, Zhang LM, Guo CY, Xu M. 2017A.** DE NOVO transcriptome sequencing
419   in passiflora edulis SIMS to identify genes and signaling pathways involved in cold tolerance. Forests **8**:
420   435.
421   **Liu Z, Jia Y, Ding Y, Shi Y, Li Z, Guo Y, Gong Z, Yang S. 2017B.** Plasma membrane CRPK1-mediated
422   phosphorylation of 14-3-3 proteins induces their nuclear import to fine-tune CBF signaling during cold
423   response. Mol Cell **66**: 117-128.
424   **Liu J, Shi Y, Yang S. 2018A.** Insights into the regulation of C-repeat binding factors in plant cold signaling. J
425   Integr Plant Biol **60**: 780-795.
426   **Liu Y, Xu C, Zhu Y, Zhang L, Chen T, Zhou F, Chen H, Lin Y. 2018B.** The calcium-dependent kinase

biblio
427   OsCPK24 functions in cold stress responses in rice. J Integr Plant Biol **60**: 173-188.

428 **Liu X, Fu L, Qin P, Sun Y, Liu J, Wang X. 2019.** Overexpression of the wheat trehalose 6-phosphate

429   synthase 11 gene enhances cold tolerance in *Arabidopsis thaliana*. Gene **710**: 210-217.

430 **Livak KJ, Schmittgen TD. 2001.** Analysis of relative gene expression data using real-time quantitative PCR

431   and the 2(-Delta Delta C(T)) Method. Methods **25**: 402-408.

432 **Love MI, Huber W, Anders S. 2014.** Moderated estimation of fold change and dispersion for RNA-seq data

433   with DESeq2. Genome Biol **15**: 550.

434 **Ma Y, Dai X, Xu Y, Luo W, Zheng X, Zeng D, Pan Y, Lin X, Liu H, Zhang D, Xiao J, Guo X, Xu S, Niu**

435   **Y, Jin J, Zhang H, Xu X, Li L, Wang W, Qian Q, Ge S, Chong K. 2015.** COLD1 confers chilling

436   tolerance in rice. Cell **160**: 1209-1221.

437 **Mann m JO. 2003.** Proteomic analysis of post-translational modifications. Nat Biotechnol **21**: 255-261.

438 **Saijo Y, Hata S, Kyozuka J, Shimamoto K, Izui K. 2000.** Over-expression of a single Ca2+-dependent

439   protein kinase confers both cold and salt/drought tolerance on rice plants. Plant J **23**: 319-327.

440 **Salzberg SL, Langmead B. 2012.** AST gapped-read alignment with bowtie 2. Nat Methods **9**: 357-359.

441 **Seong es BS, Cho hs CD. 2007.** Induction of enhanced tolerance to cold stress and disease by overexpression

442   of the pepper CAPIF1 gene in tomato. Physiol Plant **129**: 555-566.

443 **Shi J, Cao Y, Fan X, Li M, Wang Y, Ming F. 2012.** A rice microsomal delta-12 fatty acid desaturase can

444   enhance resistance to cold stress in yeast and Oryza sativa. Mol Breeding **29**: 743-757.

445 **Shi Y, Ding Y, Yang S. 2018.** Molecular regulation of CBF signaling in cold acclimation. Trends Plant Sci **23**:

446   623-637.

447 **Soto T, Beltrán FF, Paredes V, Madrid M, Millar JB, Vicente-soler J, Cansado J, Gacto M. 2002.** Cold

448   induces stress-activated protein kinase-mediated response in the fission yeast Schizosaccharomyces

449   pombe. Eur J Biochem **269**: 5056-5065.

450 **Stockinger EJ, Gilmour SJ, Thomashow MF. 1997.** *Arabidopsis thaliana* CBF1 encodes an AP2 domain-

451   containing transcriptional activator that binds to the C-repeat/DRE, a cis-acting DNA regulatory element

452   that stimulates transcription in response to low temperature and water deficit. Proc Natl Acad Sci U S A

453   **94**: 1035-1040.

454 **Su G, Morris JH, Demchak B, Bader GD. 2014.** Biological network exploration with Cytoscape 3. Curr

455   Protoc Bioinformatics **8**: 8.13.1–8.1.

456 **Teige M, Scheikl E, Eulgem T, Dóczi R, Ichimura K, Shinozaki K, Dangl JL, Hirt H. 2004.** The MKK2

457   pathway mediates cold and salt stress signaling in *Arabidopsis*. Mol Cell **15**: 141-152.

458 **Upchurch RG. 2008.** Fatty acid unsaturation, mobilization, and regulation in the response of plants to stress.

459   Biotechnol Lett **30**: 967-977.

460 **Vogel JT, Zarka DG, Van buskirk HA, Fowler SG, Thomashow MF. 2005.** Roles of the CBF2 and ZAT12

461   transcription factors in configuring the low temperature transcriptome of *Arabidopsis*. Plant J **41**: 195-211.

462 **Wang DZ, Jin YN, Ding XH, Wang WJ, Zhai SS, Bai LP, Guo ZF. 2017.** Gene regulation and signal

463   transduction in the ICE-CBF-COR signaling pathway during cold stress in plants. Biochemistry (Mosc)

464   **82**: 1103-1117.

465 **Wang H, Tang J, Liu J, Hu J, Liu J, Chen Y, Cai Z, Wang X. 2018.** Abscisic acid signaling inhibits

466   brassinosteroid signaling through dampening the dephosphorylation of BIN2 by ABI1 and ABI2. Mol

467   Plant **11**: 315-325.

468 **Wang X, Ding Y, Li Z, Shi Y, Wang J, Hua J, Gong Z, Zhou JM, Yang S. 2019.** PUB25 and PUB26
469   promote plant freezing tolerance by degrading the cold signaling negative regulator MYB15. Dev Cell **51**:
470   222-235.
471 **Webb MS, Uemura M, Steponkus PL. 1994.** A comparison of freezing injury in oat and rye: two cereals at
472   the extremes of freezing tolerance. Plant Physiol **104**: 467-478.
473 **Wu J, Zhang Y, Yin L, Qu J, Lu J. 2014.** Linkage of cold acclimation and disease resistance through plant-
474   pathogen interaction pathway in Vitis amurensis grapevine. Funct Integr Genomics **14**: 741-755.
475 **Wu Y, Tian Q, Huang W, Liu J, Xia X, Yang X, Mou H. 2020.** Identification and evaluation of reference
476   genes for quantitative real‑time PCR analysis in Passiflora edulis under stem rot condition. Mol Biol Rep
477   **47**: 2951-2962.
478 **Xie G, Kato H, Imai R. 2012.** Biochemical identification of the OsMKK6-OsMPK3 signalling pathway for
479   chilling stress tolerance in rice. Biochem J **443**: 95-102.
480 **Yadav SK. 2010.** Cold stress tolerance mechanisms in plants. Agron Sustain Dev **30**: 605-620.
481 **Yamori W, Hikosaka K, Way DA. 2014.** Temperature response of photosynthesis in C3, C4, and CAM
482   plants: temperature acclimation and temperature adaptation. Photosynth Res **119**: 101-117.
483 **Ye K, Li H, Ding Y, Shi Y, Song C, Gong Z, Yang S. 2019.** BRASSINOSTEROID-INSENSITIVE2
484   negatively regulates the stability of transcription factor ICE1 in response to cold stress in *Arabidopsis*.
485   Plant Cell **31**: 2682-2696.
486 **Yuan P, Du L, Poovaiah BW. 2018A.** Ca2+/Calmodulin-dependent AtSR1/CAMTA3 plays critical roles in
487   balancing plant growth and immunity. Int J Mol Sci **19**: E1764.
488 **Yuan P, Yang T, Poovaiah BW. 2018B.** Calcium signaling-mediated plant response to cold stress. Int J Mol
489   Sci **19**: E3896.
490 **Yue C, Cao HL, Wang L, Zhou YH, Huang YT, Hao XY, Yc W, Wang B, Yang YJ, Wang XC. 2015.**
491   Effects of cold acclimation on sugar metabolism and sugar-related gene expression in tea plant during the
492   winter season. Plant Mol Biol **88**: 591-608.
493 **Zhang J, Liu H, Sun J, Li B, Zhu Q, Chen S, Zhang H. 2012.** *Arabidopsis* fatty acid desaturase FAD2 is
494   required for salt tolerance during seed germination and early seedling growth. PLoS One **7**: e30355.
495 **Zhang Z, Li J, Pan Y, Li J, Zhou L, Shi H, Zeng Y, Guo H, Yang S, Zheng W, Yu J, Sun X, Li G, Ding Y,**
496   **Ma L, Shen S, Dai L, Zhang H, Yang S, Guo Y, Li Z. 2017A.** Natural variation in CTB4a enhances
497   rice adaptation to cold habitats. Nat Commun **8**: 14788.
498 **Zhang Z, Li J, Li F, Liu H, Yang W, Chong K, Xu Y. 2017B.** OsMAPK3 phosphorylates
499   OsbHLH002/OsICE1 and inhibits its ubiquitination to activate OsTPP1 and enhances rice chilling
500   tolerance. Dev Cell **43**: 731-745.
501 **Zhang F, Lu K, Gu Y, Zhang L, Li W, Li Z. 2020.** Effects of low-temperature stress and brassinolide
502   application on the photosynthesis and leaf structure of tung tree seedlings. Front Plant Sci **10**: 1767.
503 **Zhao C, Wang P, Si T, Hsu CC, Wang L, Zayed O, Yu Z, Zhu Y, Dong J, Tao W, Zhu JK. 2017A.** MAP
504   kinase cascades regulate the cold response by modulating ICE1 protein stability. Dev Cell **43**: 618-629.
505 **Zhao C, Wang P, Si T, Hsu CC, Wang L, Zayed O, Yu Z, Zhu Y, Dong J, Tao W, Zhu JK. 2017B.** Map
506   kinase cascades regulate the cold response by modulating ICE1 protein stability. Dev Cell **43**: 618-629.

Statistical results of transcriptome sequencing

Table 1 Statistical results of transcriptome sequencing

Sample	Reads number	Total base (bp)	Q30 (%)	GC content (%)
HJGA1	46599672	6989950800	93.02	45.36
HJGA2	44522400	6678360000	93.08	44.49
HJGA3	46642622	6996393300	93.23	45.31
TN1A1	47166760	7075014000	93.18	45.23
TN1A2	43505726	6525858900	93.31	44.33
TN1A3	45058566	6758784900	93.16	43.83
HJGB1	44758052	6713707800	93.34	43.83
HJGB2	43843522	6576528300	93.43	44.70
HJGB3	39087142	5863071300	93.14	43.37
TN1B1	49306634	7395995100	93.31	45.51
TN1B2	44267228	6640084200	93.17	44.87
TN1B3	39177250	5876587500	93.27	44.89

Sequencing data mapped to unigene set

Table 2 Sequencing data mapped to unigene set

Sample	Pair reads	Aligned concordantly 0 times	Aligned concordantly exactly 1 time	Aligned concordantly >1 times	Total alignment ratio (%)
HJGA1	23299836	6183910	15486803	1629123	83.19
HJGA2	22261200	6461646	14313504	1486050	81.73
HJGA3	23321311	7002139	14768806	1550366	81.04
TN1A1	23583380	8597970	13025983	1959427	75.69
TN1A2	21752863	7919003	11974898	1858962	75.79
TN1A3	22529283	7817813	12764435	1947035	77.11
HJGB1	22379026	6946292	14131411	1301323	78.91
HJGB2	21921761	6859052	13821399	1241310	78.45
HJGB3	19543571	5267390	12862365	1413816	81.72
TN1B1	24653317	9000336	13737412	1915569	74.21
TN1B2	22133614	8908390	11548761	1676463	70.83
TN1B3	19588625	6676080	11320050	1592495	75.95

Unigenes were annotated to 7 databases

2 **Table 3 Unigenes were annotated to 7 databases**

Database	Annotated number	Annotated ratio (%)
GO	17123	36.16
KEGG	16086	33.97
KOG	23164	48.92
NR	46369	97.92
Pfam	29091	61.43
Swiss-Prot	33337	70.40
TrEMBL	46323	97.82
Total	47353	100

Figure 1

Annotation of passion fruit transcriptome

(A) GO function classification diagram of unigenes. The x-axis indicates the secondary classification terms of GO; the y-axis indicates the number of unigenes in this secondary classification out of the total annotated unigenes. (B) KOG functional annotation distribution of unigenes. The x-axis indicates the nuber unigens; the y-axis indicates the name of 25 groups. (C) KEGG classification of unigenes. The x-axis indicates the number of unigenes in the pathway; the y-axis indicates KEGG pathways.
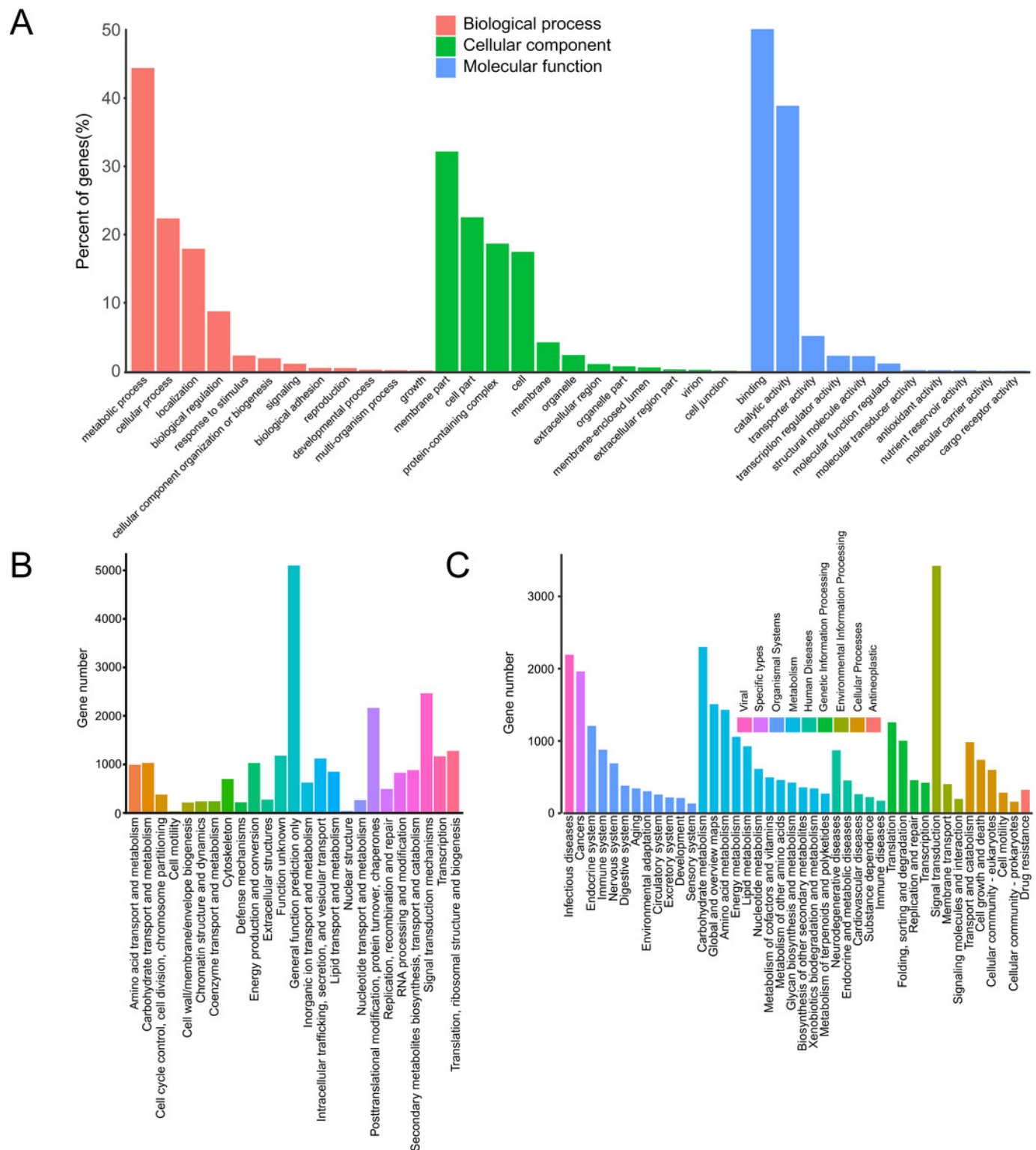
Figure 2

Analysis of DEGs at two stages.

(A) DEGs identified between HJG and TN1. (B) A1 vs A2; (C) B1 vs B2. Red indicates that the gene is highly expressed in the sample; blue indicates lower expression, and the number label under the color bar at the upper left is the specific trend of the change of expression. The left is a dendrogram of gene clustering, and below is the name of the samples. Figure 3 **KEGG pathway enrichment of DEGs.** (A) A1 vs A2. (B) B1 vs B2. The left is the name of pathways, and below is the enrichment factor. The size of the dots indicate the number of genes in this pathway, and the color of the dots corresponds to different −log10(correct p value) ranges.
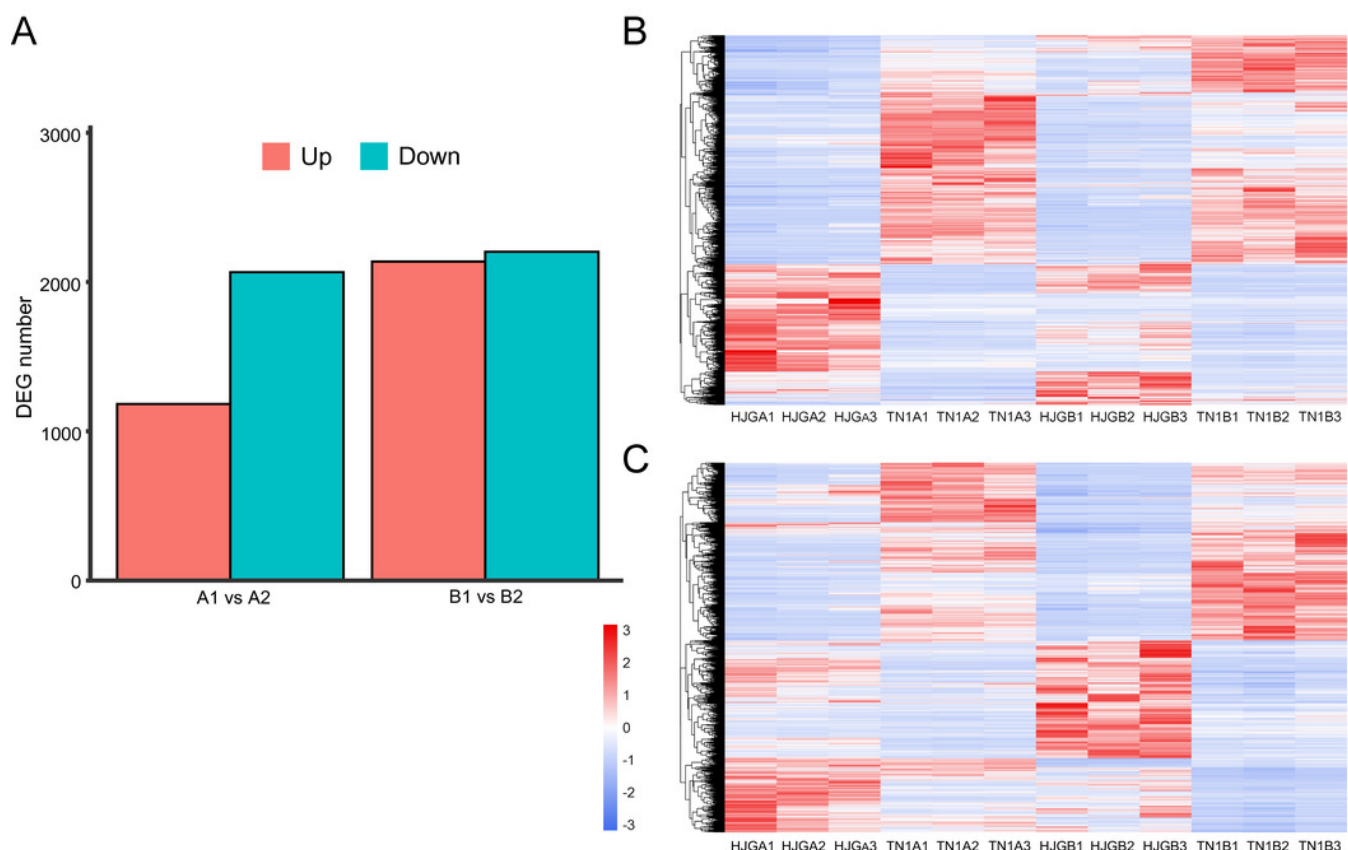
Figure 3

KEGG pathway enrichment of DEGs.

(A) A1 vs A2. (B) B1 vs B2. The left is the name of pathways, and below is the enrichment factor. The size of the dots indicate the number of genes in this pathway, and the color of the dots corresponds to different −log10(correct p value) ranges.
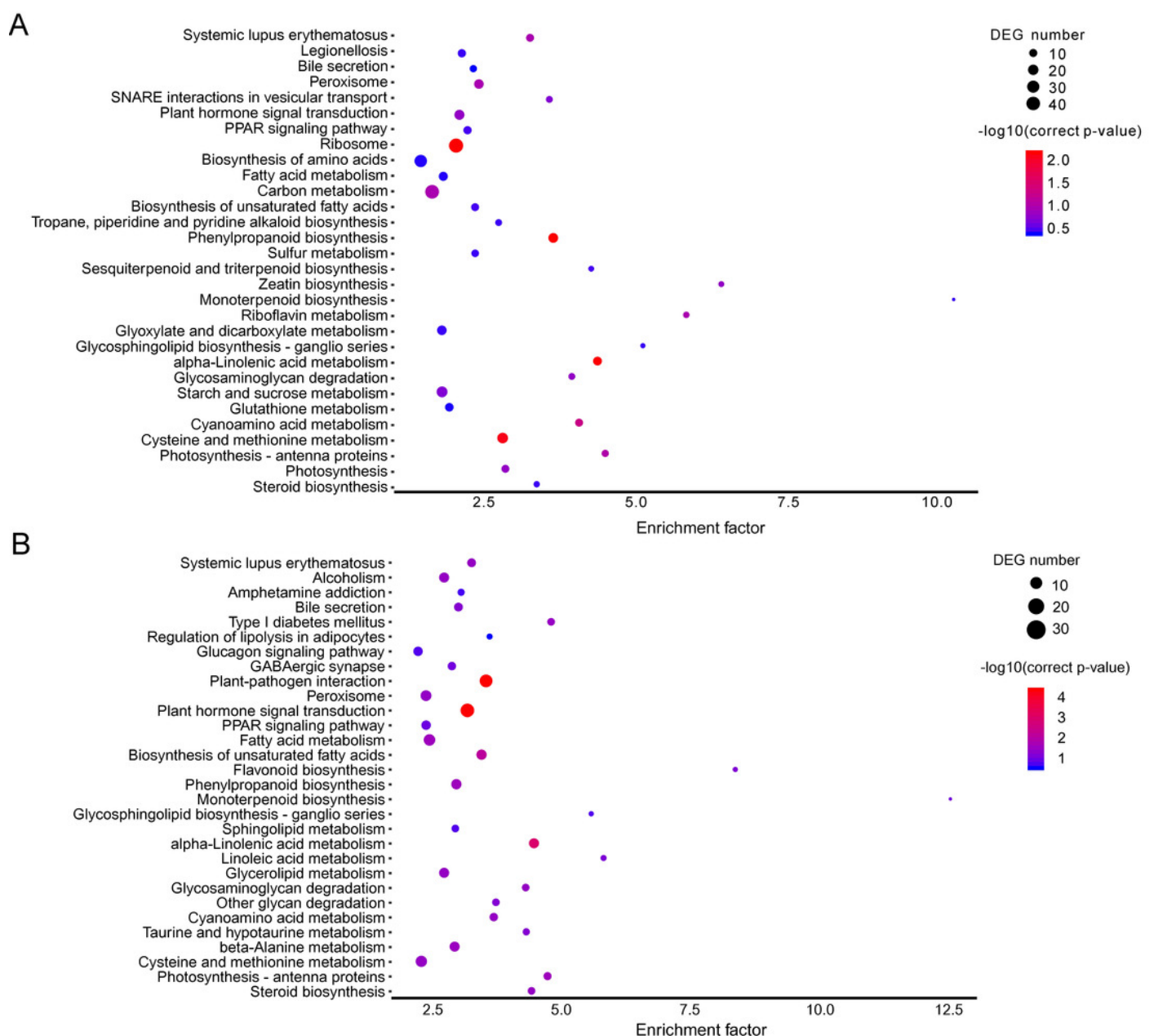
Figure 4

Thr heat map of DEGs at two stages.

(A) A1 vs A2. (B) B1 vs B2. The below is the name of the samples. Red indicates that the gene is highly expressed in the sample; blue indicates lower expression, and the number label under the color bar at the upper left is the specific trend of the change of expression.
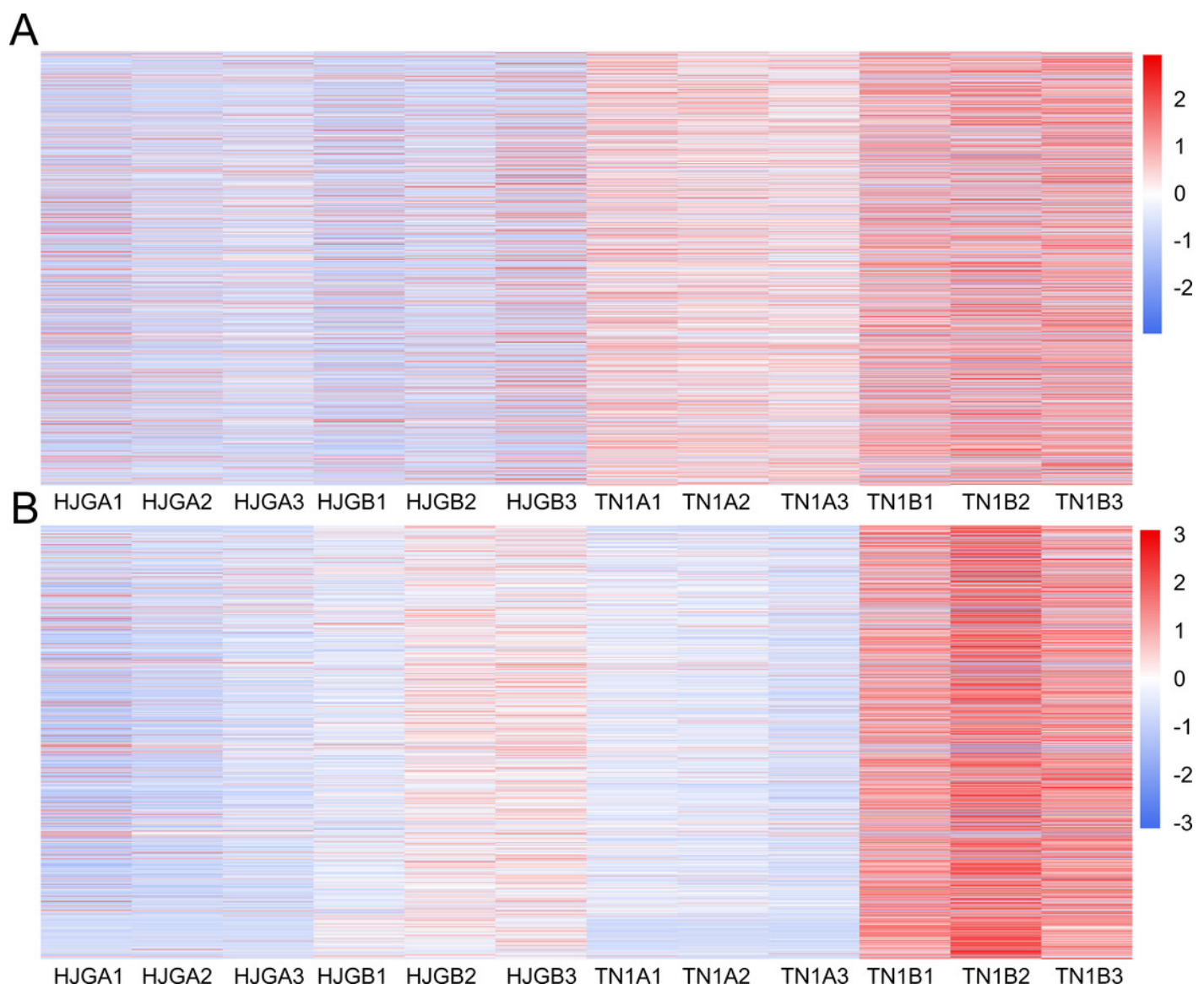
Figure 5

KEGG pathway enrichment in two co-expression modules.

(A) Brown module. (B) Yellow module. The x-axis indicates the enrichment factor; the y-axis indicates the name of pathways. The size of the dots indicate the number of genes in this pathway, and the color of the dots corresponds to different −log10 (correct p value) ranges.
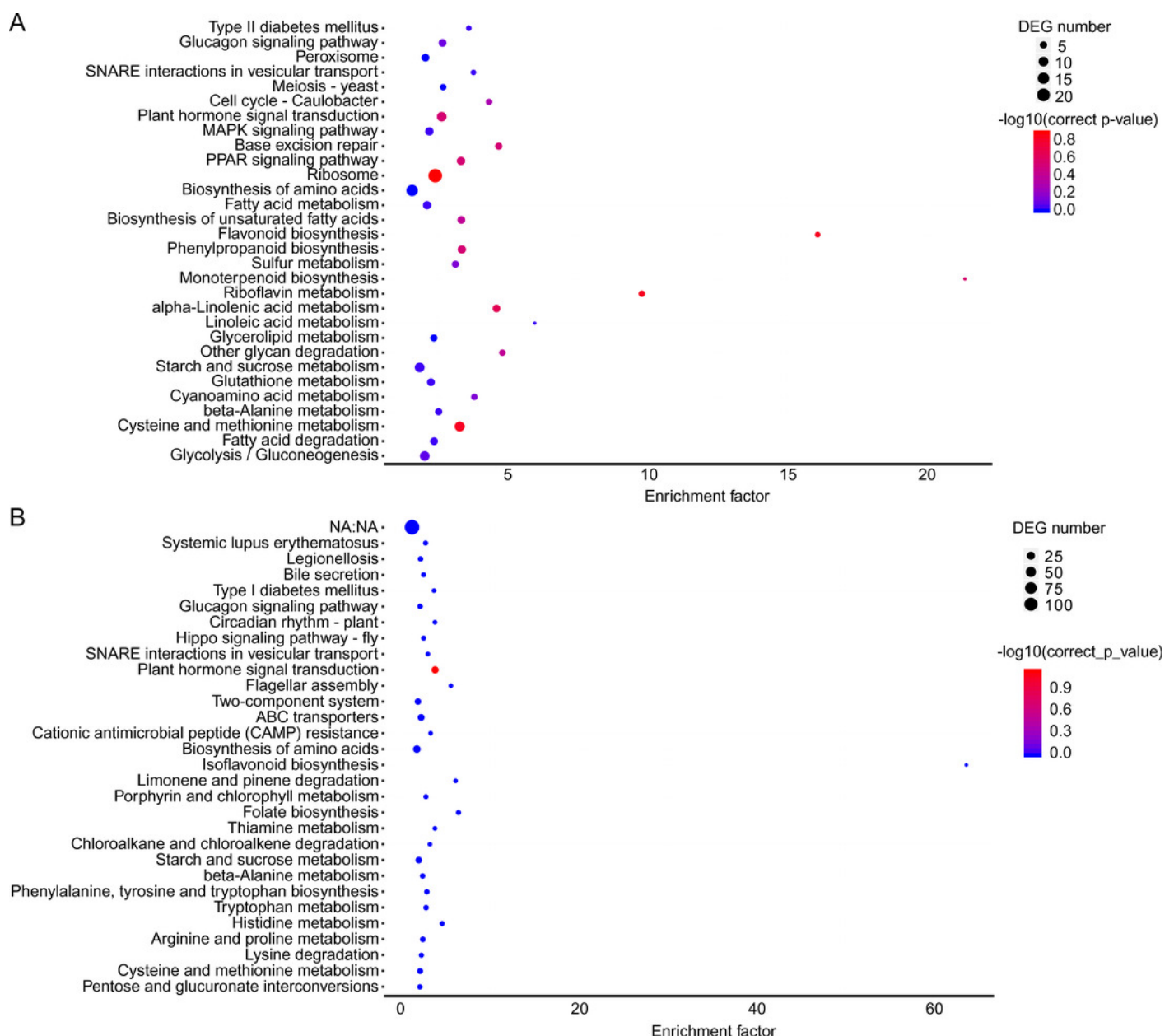
Figure 6

Gene coexpression network related to cold stress.

(A) Gene co-expression network related to cold stress in brown module. (B) Gene co-expression network related to cold stress in yellow module. Red dots represent the hube gene belonging to the co-expression network.
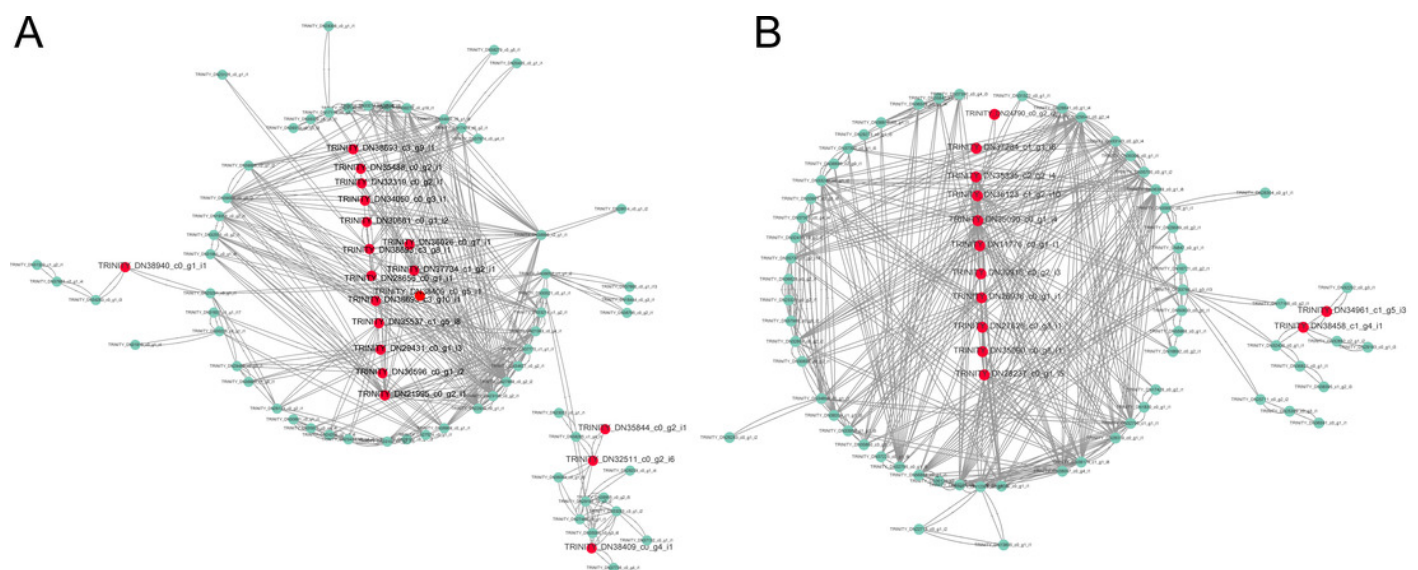
Figure 7

Cold acclimation related genes were validated by RT-qPCR.

The blocks indicate the samples of HJG and TN1 using in RT-qPCR and RNA-seq under cold stress condition. Bars indicate standard deviations of three biological repetitions.